

Kinematic Characteristics of Vertical Runner and Numerical Simulation Analysis of Rock Breaking

Jirui Li^{1, a}, Yingxin Yang^{1, b, *}

¹School of Southwest Petroleum University, Chengdu, Sichuan 610500, China
^a674872490@qq.com, ^byangyx36@qq.com
Corresponding author: Yingxin Yang

Abstract: In order to solve the problems of PDC teeth easy to collapse and fail in hard, hard and soft interlaced formations and gravel bearing formations, low mechanical speed, and difficult orientation caused by high torque response of pdc bits in directional drilling, this paper proposes a new type of composite bit with vertical wheels on the blade. Through theoretical analysis, the rotating conditions of the vertical wheel are obtained, that is, the contact angle of the cutting teeth of the vertical wheel must be greater than the center angle of its two adjacent teeth. At the same time, the cutting tracks generated by the previous vertical wheel unit experiments are analyzed, and the causes of different cutting tracks are obtained. Finally, the rock breaking of the PDC teeth under the pre damage of the vertical wheel is numerically simulated and analyzed, and it is concluded that the force on the PDC teeth is closely related to the relative height between the cutting teeth of the vertical wheel, It increases with the increase of relative height. When the relative height is 2mm, the tangential force on the PDC tooth is 4.78 times that when the relative height is 0mm, and the axial force is 2.47 times that when the relative height is 0mm. At the same time, the relationship between the force on the PDC teeth and the normal deflection angle and the rake angle of the vertical roller is not obvious.

Keywords: PDC cutting teeth, Vertical wheel, Rotating conditions, Cutting track, Relative height.

1. Introduction

The focus of oil and gas exploration and development in China has shifted to deep/deep water/unconventional oil and gas (including shale gas).[1] The technical innovation of bit is one of the most promising efforts to improve the drilling speed in deep formation. [2]The most widely used bit in oil and gas drilling is polycrystalline diamond composite bit, that is, PDC (Polycrystalline Diamond Compact) bit. This bit has the advantages of high rock breaking efficiency, high penetration rate and long working life in medium hard formations.[3] However, its drilling speed is slow, its service life is low, and its stability is poor when drilling into deep and hard to drill formations such as strong plasticity, gravel and interlayer.[4] In view of this situation, the bit laboratory of Southwest Petroleum University proposed a vertical wheel PDC bit. Its structure is shown in Figure 1. It combines the runner and bearing and applies them to the PDC bit, forming a new technology of vertical wheel PDC bit. The theoretical analysis and experimental test results show that the setting of the vertical runner has the functions of auxiliary cutting, partial pressure buffering and torque stabilizing, which can significantly improve the working stability of the PDC bit and reduce the wear rate of the bit cutting teeth.[5] However, the precondition for the vertical roller PDC bit to achieve the above functions is that the vertical roller can rotate smoothly when working at the bottom of the well. Therefore, the rotating conditions of the vertical roller are very important for the design of the vertical roller PDC bit. The vertical wheel PDC bit introduces a vertical runner on the conventional fixed cutting bit. Compared with the conventional PDC bit, the runner structure is placed on the PDC main blade, which works with the PDC fixed blade. The pre breaking of the runner on the rock will greatly reduce the difficulty of PDC cutting teeth in cutting the rock and improve the performance

of the bit. In order to quantitatively study the rock breaking effect of the combined action of the cutting teeth and PDC teeth of the runner and conduct numerical simulation, the main position parameters of the runner are analyzed, including the normal angle of the runner α 、 Front inclination γ And the influence of the relative the PDC tooth on the stress of the PDC tooth

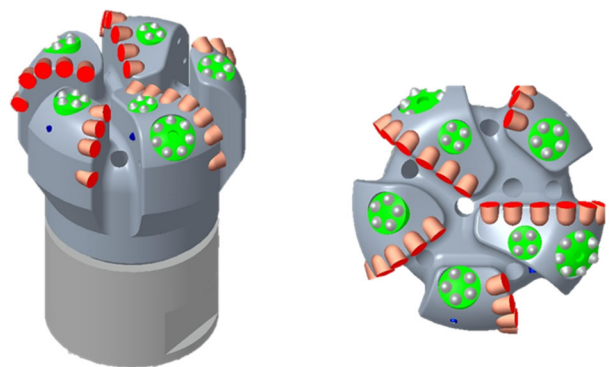


Figure 1. Structural Diagram of Vertical Wheel PDC Bit

2. Rotating Conditions of Vertical Runner Rotating Conditions of Vertical Runner

As shown in Fig. 1 (a), it represents the position diagram of A tooth and B tooth when the runner rotates clockwise and A tooth just contacts the rock. At this time, the vertical height of B tooth from the rock surface is m . Figure 1 (b), The adjacent subsequent cutting teeth can eat into the rock. Figure 1 (c) shows the height L of the B tooth descending perpendicular to the rock surface during the process of A tooth contacting the rock at the beginning and leaving the rock. According to the above critical rotating conditions of the

runner, the rotating conditions of the runner are:

$$L \geq m \quad (1)$$

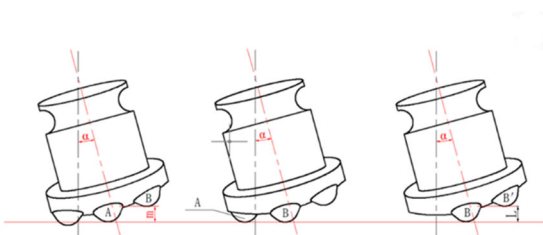


Figure 2. Schematic Diagram of Rotating Conditions of Runner

2.1. Find the Value of m

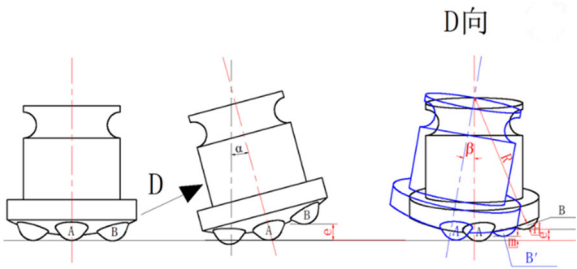


Figure 3. Diagram of relationship between m value and normal deflection angle and front inclination angle

Figure 3 (a) shows the schematic diagram of the runner without normal deflection angle and rake angle. At this time, the vertical height of B tooth from the rock is 0. Figure 3 (b) shows that the normal inclination of the runner is α . The vertical height of tooth B from the rock is e . Figure 3 (c) shows that the normal deflection angle of the runner is α . It also has a front inclination angle β . The vertical height of tooth B from rock decreases from e to m .

As shown in Figure 3 (b) and Figure 4:

$$e = 2r \sin \theta \sin \alpha \quad (2)$$

Where R is the radius of the top circle of the runner cutting tooth, θ is the center angle between A and B teeth, α is the normal deflection angle.

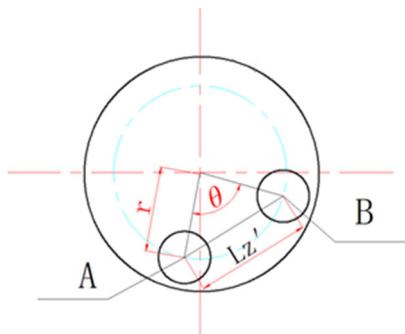


Figure 4. Schematic diagram of e value

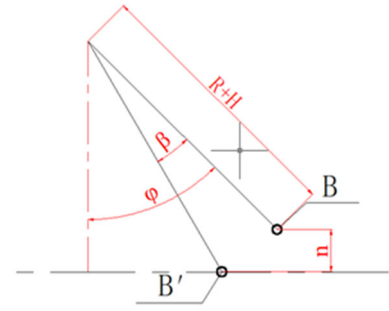


Figure 5. Schematic diagram of m value

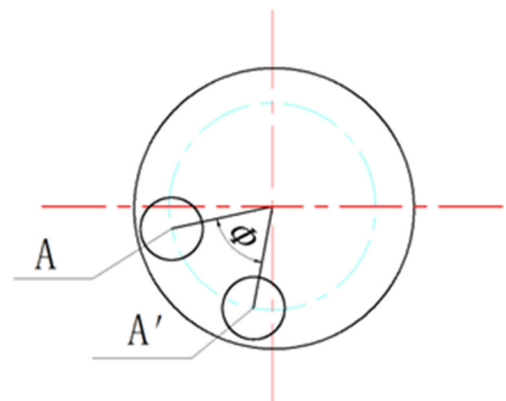
As shown in Figure 2 (c) and Figure 5:

$$m = e - n \quad (3)$$

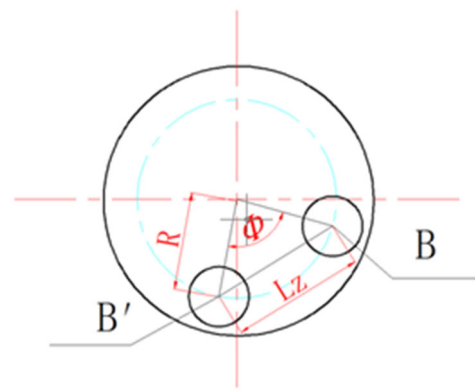
$$n = (R + H) \times [\cos(\varphi - \beta) - \cos(\varphi)] \quad (4)$$

$$m = 2r \sin \theta \sin \alpha - (R + H) \times [\cos(\varphi - \beta) - \cos(\varphi)] \quad (5)$$

Where R is the contour radius of the runner tooth surface, and H is the exposed height of the cutting teeth



(a)



(b)

Figure 6. Schematic diagram of L value and A gear rotation angle

2.2. Finding the Value of L

Figure 6 (a) shows that the cutting tooth starts to contact the rock at A' position, and when it reaches A position, the cutting tooth leaves the rock. In this process, the rotation angle of the cutting tooth A is Φ . Then the cutting tooth B turns at an angle of φ . In this process, the height L of B tooth descending in the direction perpendicular to the rock:

$$L = 2r\sin\Phi\sin\alpha - (R + H) \times [\cos(\varphi - \beta) - \cos(\varphi)] \quad (6)$$

The calculation process is the same as the above principle. Since its rotation condition is $L \geq m$

$$2r\sin\Phi\sin\alpha - (R + H) \times [\cos(\varphi - \beta) - \cos(\varphi)] \geq 2r\sin\theta\sin\alpha - (R + H) \times [\cos(\varphi - \beta) - \cos(\varphi)] \quad (7)$$

Get:

$$\Phi \geq \theta \quad (8)$$

Therefore, the condition for the runner to rotate is that the contact angle of the cutting teeth of the runner must be greater than the center angle of the two adjacent teeth.

2.3.1 Find Contact Angle Φ Value of When Only Normal Deflection Angle Exists

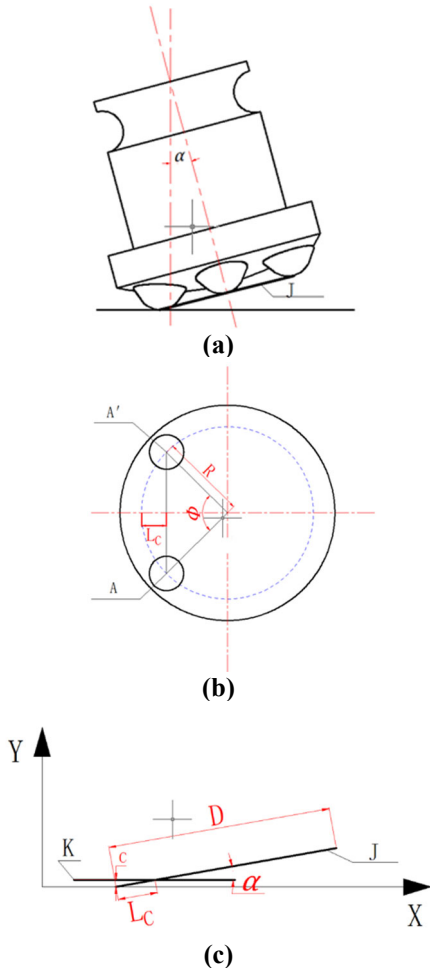


Figure 7. seek Φ Schematic Diagram of Value Location

As shown in Fig.7 (a), J represents the tooth tip circular plane of the runner cutting teeth. We assume that the tooth tip feature point of each cutting tooth is prior to the rock contact. When the tooth penetration depth is C, the sketch map of the intersection between the tooth top circle plane and the rock plane is shown in Figure 7 (c), where K represents the rock plane, and the line segment LC represents the projection length of the part of the tooth top circle intersecting the rock in the cutting direction. Its length in the top view of the runner is shown in Figure7 (b), so it can be seen from Figure 7 (c) that:

$$L_c = \frac{c}{\sin\alpha} \quad (9)$$

From Figure 7 (b):

$$\Phi = 2 \cos^{-1} \left(1 - \frac{c}{R \sin\alpha} \right) \quad (10)$$

Therefore, under ideal conditions, as long as $2 \cos^{-1} \left(1 - \frac{c}{R \sin\alpha} \right) \geq \theta$, The wheel can turn.

2.3.2 When Normal Deflection Angle and Front Inclination Angle Exist Simultaneously

As shown in Figure 8, The geometric coordinate system of the vertical wheel includes three rectangular coordinate systems with the spherical center of the runner tooth surface as the origin. They are respectively the position coordinate system $O_1X_1Y_1Z_1$; Normal declination coordinate system $O_1X_2Y_2Z_2$; Tilt forward coordinate system or working coordinate system $O_1X_3Y_3Z_3$.

Plane $O_1X_1Z_1$ Center plane of runner, coordinate axis O_1Z_1 Perpendicular to the rock plane, O_1Y_1 Axis pointing to O_1 Speed direction at 1 point. Set $O_1X_1Y_1Z_1$ Coordinate system around O_1Y_1 axis rotation α After the angle, O is formed $O_1X_2Y_2Z_2$ Coordinate system. Set $O_1X_2Y_2Z_2$ Coordinate system around O_1X_2 -axis rotation- β After the angle, O is formed $O_1X_3Y_3Z_3$ Coordinate system.

When the normal deflection angle and the rake angle exist at the same time, the contact angle between the cutting teeth of the runner and the rock is required, which is actually the intersection point between the tooth tip circle of the cutting teeth of the runner and the rock plane. The contact angle is the center angle between the two intersection points.

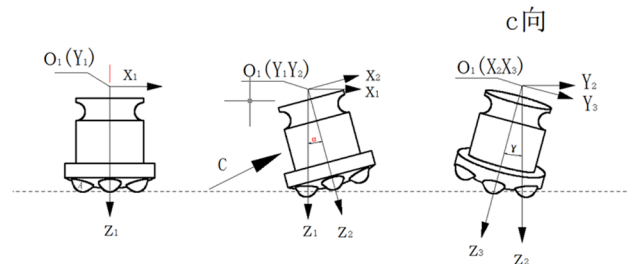


Figure 8. Coordinate system of vertical roller

At $O_1X_3Y_3Z_3$, the equation of the addendum circle can be

expressed as:

$$\begin{cases} x_3^2 + y_3^2 = R^2 \\ Z_3 = K \end{cases} \quad (11)$$

Where, R represents the radius of the addendum circle, and K represents the distance from the plane of the addendum circle to O_1 The height of 1 point. Through coordinate transformation, the equation of addendum circle can be obtained in coordinate system $O_1X_1Y_1Z_1$ The specific steps of the expression in 1 are as follows:

Rotate around X axis β :

$$\begin{aligned} x_3 &= x_2 \\ y_3 &= y_2 \cos \beta - z_2 \sin \beta \\ z_3 &= y_2 \sin \beta + z_2 \cos \beta \end{aligned} \quad (12)$$

Rotate around y-axis- α

$$\begin{aligned} x_2 &= z_1 \sin \alpha + x_1 \cos \alpha \\ y_2 &= y_1 \\ z_2 &= z_1 \cos \alpha + x_1 \sin \alpha \end{aligned} \quad (13)$$

From the above formula, we can get:

$$\begin{aligned} x_3 &= z_1 \sin \alpha + x_1 \cos \alpha \\ y_3 &= y_1 \cos \beta - (z_1 \cos \alpha + x_1 \sin \alpha) \sin \beta \\ z_3 &= y_1 \sin \beta + (z_1 \cos \alpha + x_1 \sin \alpha) \cos \beta \end{aligned} \quad (14)$$

So the equation of the addendum circle is in the coordinate system $O_1X_1Y_1Z_1$ The expression in 1 is:

$$\begin{cases} (z_1 \sin \alpha + x_1 \cos \alpha)^2 \\ + [y_1 \cos \beta \\ - (z_1 \cos \alpha - x_1 \sin \alpha) \sin \beta]^2 = R^2 \\ y_1 \sin \beta + (z_1 \cos \alpha + x_1 \sin \alpha) \cos \beta = k \end{cases} \quad (15)$$

Then the intersection point between the tooth tip circle and the rock plane is:

$$\begin{cases} (z_1 \sin \alpha + x_1 \cos \alpha)^2 \\ + [y_1 \cos \beta \\ - (z_1 \cos \alpha - x_1 \sin \alpha) \sin \beta]^2 = R^2 \\ y_1 \sin \beta + (z_1 \cos \alpha + x_1 \sin \alpha) \cos \beta = k \\ Z_1 = k - C \end{cases} \quad (16)$$

Wherein, C is the eating depth of the cutting tooth, and the above equations can be used to solve x_1 , y_1 , the contact angle of the cutting teeth of the runner can be obtained.

3. Factors Influencing the Cutting Path of Runner

Yang Yan [5] carried out unit experiment research on rock breaking of runner, and analyzed the movement law and rock breaking characteristics of runner under different rake angle, normal deflection angle, runner height, tooth shape and

runner diameter. However, she did not find out the internal causes of various cutting trajectories. Therefore, based on Yang Yan, this paper analyzes the causes of various cutting trajectories in detail.

In order to better describe the cutting track, the track length l , track width w and track spacing d are introduced, as shown in Figure 9.

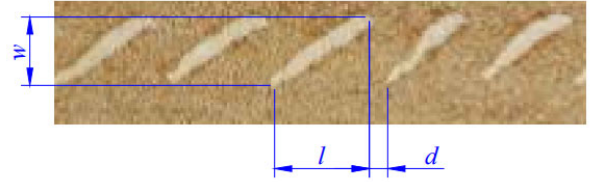


Figure 9. Cutting track parameters

As shown in Figure 10, in the unit experiment of the runner, the top point of the cutting tooth of the runner is taken as the moving point, the runner is the dynamic coordinate system, and the rock is the static coordinate system. Then the motion of the moving point relative to the rock is absolute motion, and the trajectory is a complex spatial curve motion; The motion of the moving point relative to the runner is a relative motion, and its trajectory is a circle, while the motion of the runner relative to the rock is a drag motion, which is a linear translation of the rigid body. The relative velocity v of moving point v_r is decomposed into v_{rxy} and v_{rz} where v_{rxy} is the relative velocity v_r . The projection of on the XOY plane v_{rxy} is decomposed along the x and y axes to obtain v_x and v_y . Then the displacement corresponding to the track length in the cutting track is the speed v_c related, track width and relative velocity v_r . The component of the projection of on the xoy plane along the x-axis v_x , the depth of the trajectory perpendicular to the rock plane is related to v_{rz} correlation.

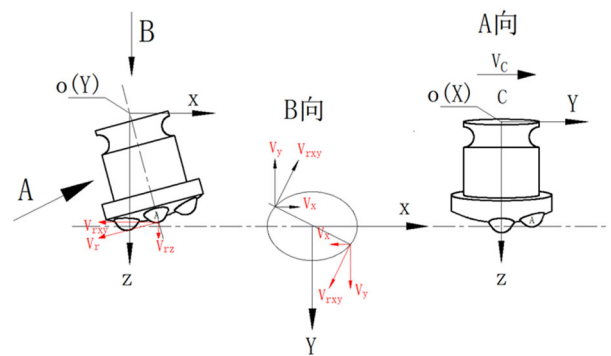


Figure 10. Speed breakdown of runner cutting teeth

The length of the track is determined by the contact time between the cutting teeth and the rock and the implicated speed of the runner, while the width of the track is determined by the contact time between the cutting teeth and the rock, the track width and the relative speed v . The component v of the projection of r on the xoy plane along the x-axis v_x is relevant. The distance between tracks is related to the length of tracks and the distance between adjacent teeth.

3.1. Influence of Normal Deflection Angle on Cutting Path:

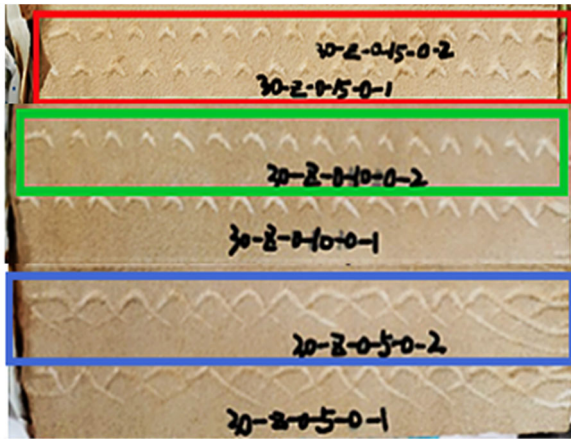


Figure 11. Schematic diagram of the influence of normal deflection angle on cutting path

As shown in Figure 11, the red, green and blue boxes respectively represent the normal deflection angles of 15 °, 10 ° and 5 °. The cutting path shape of tapered tooth is "V" when only normal deflection angle exists. As the normal deflection angle increases, the length and width of the trace line will be shorter, and the spacing between the trace lines will be smaller. This is because when there is only the normal deflection angle, the two intersection points of the top circle of the runner and the rock plane are the positions where the cutting teeth start to contact the rock and leave the rock. The vertical planes of the two intersection points pass through the center of the top circle and are parallel to the axis of the runner. The intersection point of the vertical plane and the top circle is the farthest that the cutting teeth can reach. Horizontal position. When you turn this point, the direction of the trajectory line will "turn back". With the increase of the normal deflection angle, the contact angle between the cutting teeth on the runner and the rock decreases gradually. Because the rotation speed of the runner is less affected by the normal deflection angle, the larger the normal deflection angle is, the shorter the action time between the cutting teeth on the runner and the rock, the shorter the length of the trajectory, and the smaller the width of the trajectory. The position where the two adjacent teeth start to contact the rock is independent of the normal deflection angle, so the distance between the positions where the two adjacent teeth just start to contact the rock in the track is equal. The greater the normal deflection angle is, the shorter the track line length is, so the distance between the two adjacent track lines is longer.

3.2. Effect of Rake Angle on Cutting Path

As shown in Figure 11, when there is both normal deflection angle and rake angle, the shape of the track becomes oblique because the rake angle is added, so that the tooth top circular plane of the runner rotates an angle around the mid vertical plane of the two intersection points, which is equal to the magnitude of the rake angle. The vertical height of the tooth top circle in the front half of the vertical plane to the rock is lower, while the vertical height of the back half of the vertical plane to the rock is higher. At this time, the two intersection points of the top circle of the runner tooth and the rock plane are no longer symmetrical with respect to the vertical plane, and the position of the cutting tooth leaving the

rock changes from the back half of the vertical plane to the front half of the vertical plane. Therefore, the trace line has no "turning back" shape. At the same time, the increase of the length and width of the trace line is due to, on the one hand, the rake angle makes the contact angle of the cutting teeth larger, and on the other hand, the addition of the rake angle makes the speed of the runner slower. Therefore, the superposition of the two makes the length and width of the trace line increase. The increase of the length of the trace line makes the distance between the two trace lines smaller.

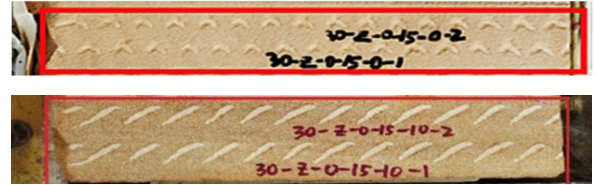


Figure 12. Diagram of influence of rake angle on cutting path

3.3. Effect of Runner Diameter on Cutting Path

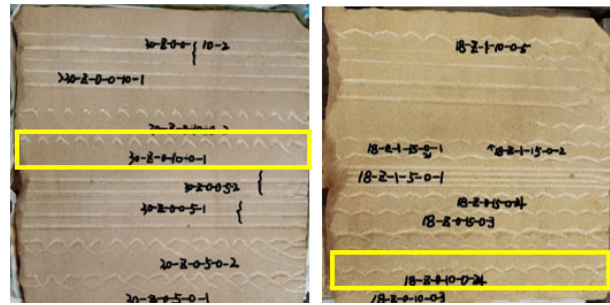


Figure 13. Schematic diagram of influence of runner diameter on cutting path

The contact angle of the cutting teeth of the runner decreases with the increase of the runner diameter, and the average speed of the runner also decreases with the increase of the runner diameter. However, after calculation, when there is only normal deflection angle, the contact time between cutting teeth and rock decreases with the increase of runner diameter. Therefore, as shown in the figure, the track line length of the 18mm runner is longer than that of the 30mm runner. But in the transverse direction, due to the component v of the relative velocity in the Y-axis direction, the width change of cutting path is not obvious under the joint influence of v_{ry} and contact time.

3.4 Effect of Cutting Depth on Cutting Path

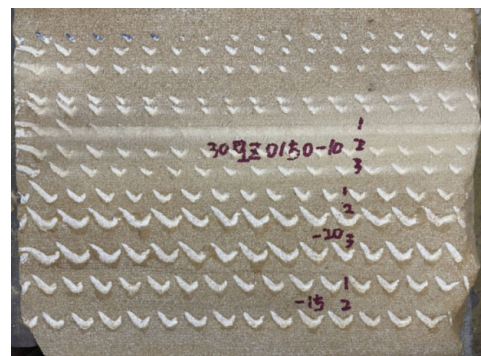


Figure 14. Schematic Diagram of the Influence of Cutting Depth on Cutting Path

With the increase of the depth of penetration, the contact angle of the cutting teeth also increases, so the contact time also increases, so the length and width of the trajectory line increase, and at the same time the spacing between the tracks becomes smaller.

3.5 Influence of Cutting Tooth Profile on Cutting Path

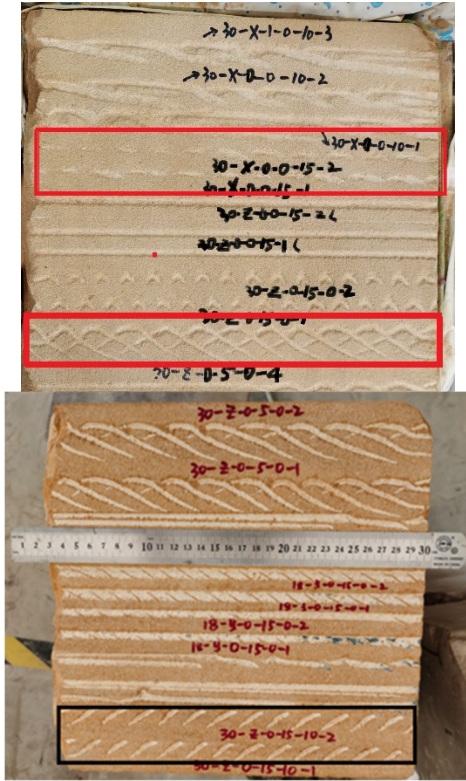


Figure 15. Comparison Diagram of Wedge Tooth, Taper Tooth and Steel Tooth Tracks

Wedge tooth, tapered tooth and steel tooth with two section shapes, when the normal deflection angle Δ is the same $\gamma =$ When the angle is 15° , the cutting path of the wedge tooth on the runner is "straight", the cutting path of the cone tooth is "V", and the cutting path of the steel tooth is "oblique". The length l of the cutting path of the wedge tooth is the longest, the width w is the widest, and the spacing d of the cutting path of the steel tooth is the smallest.

4. Numerical Simulation Analysis of Rock Breaking Under Pre Damage of Vertical Runner

4.1. Establishment of Geometric Model

Based on ABAQUS software, this paper analyzes the

microscopic interaction between the runner rock system. [6]The runner diameter is 30mm (taking the distance from the tip of the runner to the runner shaft as the radius). The hard alloy tapered teeth are used on the runner. The diameter of the teeth is 9mm, the diameter of the PDC teeth is 15.7mm, the tooth thickness is 7.5mm, the rake angle is 5° , and the side angle is 0° . Because of the irregular shape of the teeth and runner body, their grids are C3D10M; [7] Rock size is $80\text{mm} \times 80\text{mm} \times 40\text{mm}$, the 8-node linear hexahedral reduced integral element (C3D8R) with hourglass control is used for discretization, and the local grid of rock is refined, as shown in Figure 3. Fixed constraints are imposed on the bottom of the rock, and symmetrical constraints are imposed on the symmetrical plane respectively. The fastest cutting speed of the runner is 0.3m/s, which increases linearly according to a certain amplitude. The simulation time is 0.3s. The rock property is yellow sandstone, the density is 2.08g/cm^3 , the compressive strength is 21.49Mpa, the elastic modulus is 2.46Gpa, Poisson's ratio is 0.085, the internal friction angle of the rock is 22.87° , and the fracture strain is 0.0134.

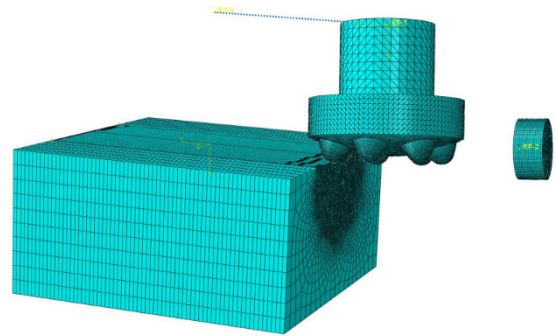


Figure 16. Simulation model of runner pre crushing

4.2. Analysis of Simulation Results

4.2.1. Influence of Relative Height

In this group of simulation experiments, the normal deflection angle of the runner is 20° , and the cutting depth of the cutting teeth of the runner is fixed at 1mm. The rake angle of the PDC gear is 5° , and the side angle is 0° . As shown in Figure 17, Changing the cutting depth of the PDC gear, five groups of simulation experimental data are obtained, and their relative heights are respectively 0, 0.5, 1, 1.5, and 2 mm. The simulation results are shown in the figure below. The axial force and tangential force of PDC cutting teeth increase with the increase of relative height. The relative height increases from 0 mm to 2 mm, the tangential force increases from 24.57 N to 142.18 N, an increase of 4.78 times, and the axial force increases from 6.68 to 23.88, an increase of 2.47 times. It can be seen that the force of PDC teeth is more sensitive to the change of relative height. The lower the relative height is, the more obvious the role of vertical wheel in auxiliary cutting is.

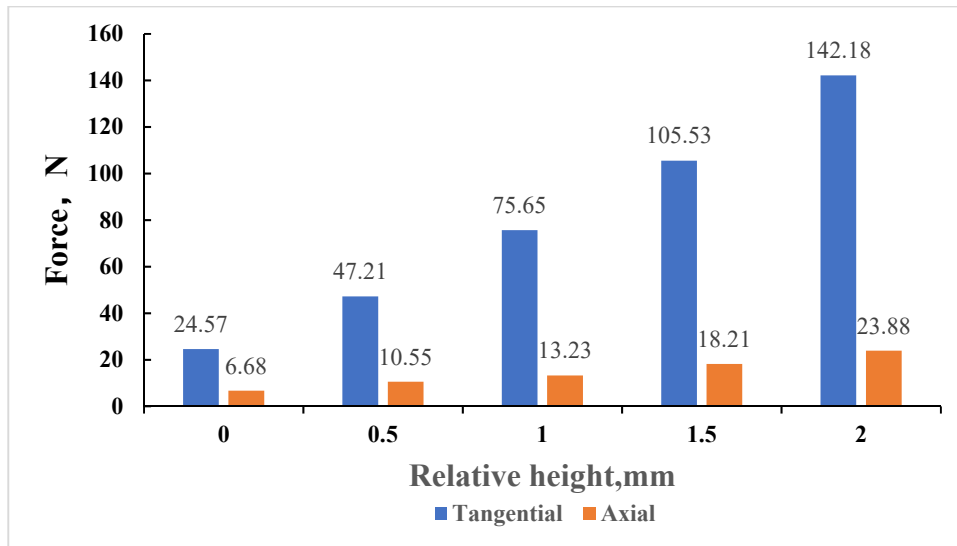


Figure 17. Schematic Diagram of Forces on Cutting Teeth at Different Relative Heights

4.2.2. Influence of Normal Deflection Angle

In this group of simulation experiments, the cutting depth of the runner cutting teeth and PDC cutting teeth is 1mm, and the normal deflection angles of the runner are 5°, 10°, 15° and 20° respectively. The rake angle of PDC cutting teeth is 5°, and the side angle is 0°. The simulation results are shown

in the following figure. The normal deflection angle of the runner has little effect on the force on the PDC cutting teeth. The maximum axial force of the PDC cutting teeth occurs when the normal deflection angle of the runner is 20°, and the maximum tangential force occurs when the normal deflection angle of the runner is 10°. However, the overall force on the PDC cutting teeth does not change significantly.

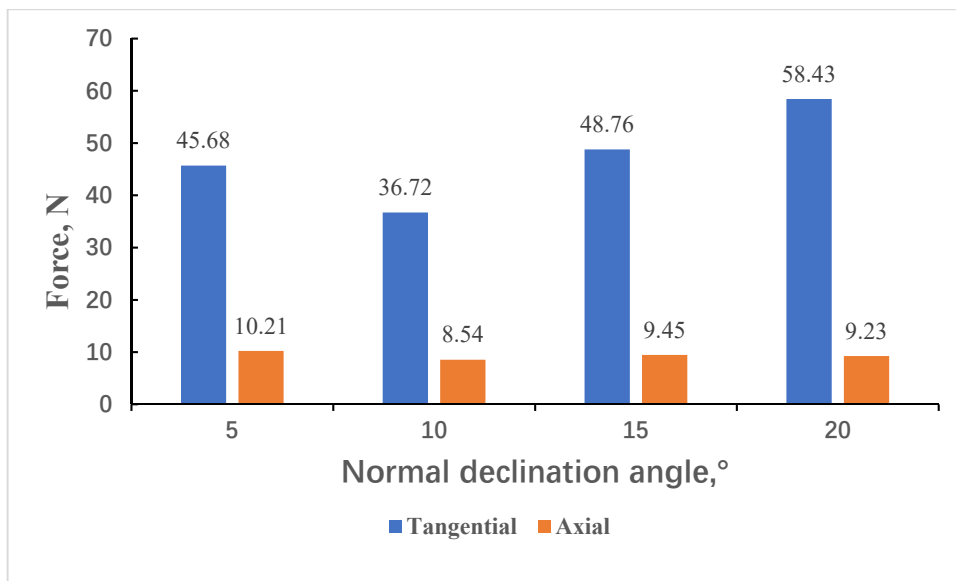


Figure 18. Force of PDC teeth under different normal deflection angles

4.2.3. Effect of Front Tilt

In this group of simulation experiments, the cutting depth of the runner cutting teeth and PDC cutting teeth is 1mm, the normal deflection angle of the runner is 20°, the variation range of the rake angle is from 5° to 20°, the rake angle of the PDC cutting teeth is 5°, and the side angle is 0°. The simulation results are shown in the figure below. The normal

deflection angle of the runner has little influence on the force on the PDC cutting teeth. The force on the PDC cutting teeth decreases first and then increases with the increase of the rake angle. When the rake angle is 10°, the axial force and tangential force are the minimum, 36.72N and 8.54N respectively.

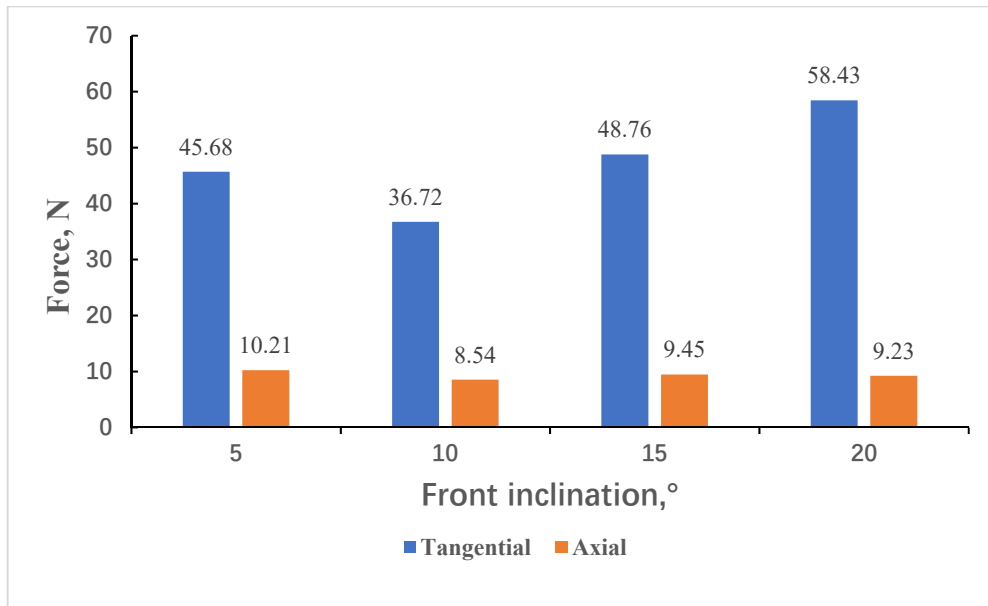


Figure 19. Force changes of PDC teeth under different rake angles

5. Conclusion

The rotating condition of vertical PDC bit is that the contact angle of the cutting teeth on the vertical wheel must be greater than the center angle of the two adjacent teeth. The contact angle of the cutting teeth of the vertical wheel is related to the normal deflection angle, the rake angle, the diameter of the vertical wheel and the eating depth of the cutting teeth.

The cutting track of the vertical wheel is essentially determined by the speed ratio of the vertical wheel body. The length of the track is determined by the contact time between the cutting teeth and the rock and the implicated speed of the runner. The width of the track is related to the contact time between the cutting teeth and the rock and the width of the track and the component of the projection of the relative speed on the xoy plane along the x-axis. The distance between tracks is related to the length of tracks and the distance between adjacent teeth.

Under the pre damage effect of the vertical wheel, the force on the PDC tooth increases with the increase of the relative height between the PDC tooth and the vertical wheel cutting tooth. The normal deflection angle of the vertical wheel has little effect, and decreases first and then increases with the increase of the rake angle. When the rake angle is 10 °, the axial force and tangential force are minimum.

References

- [1] Sun Weiwei Current situation and development trend of deep and ultra deep well drilling technology [J] Process technology 2020(9): 236-237.
- [2] Wang Yaojia, Wang Zaixing, Shen Liyang, etc Current situation and development trend of domestic deep and ultra deep well drilling technology [J] Petrochemical technology 2016, 23(02): 52.
- [3] Bai Jing, Zhang Bin, Zhang Chaoping Current situation and development suggestions of ultra deep and ultra slim hole directional drilling technology [J] Drilling and production technology 2018, 41(6): 5-8.
- [4] Zhang Jingcheng, Ma Lijun, Liu Yong, et al Research and application of ultra deep and ultra slim hole directional drilling technology in Tarim Oilfield [J] Special oil and gas reservoirs 2020, 27(02): 164-168.
- [5] Yang Yan Study on working mechanism and design method of vertical wheel PDC bit [D] Southwest Petroleum University, 2020.
- [6] Feng Yuguo Application of ABAQUS in Geotechnical Engineering [M] China Water Resources and Hydropower Press, 2013.
- [7] Wu Kaisong, Liao Feilong Discussion on rock breaking law of PDC teeth after rock cutting damage [J] Petroleum Machinery, 2014, 42 (5): 29-33.